Searching for extra Z' from strings and other models at the CERN LHC with leptoproduction

Claudio Corianò,[1,2] Alon E. Faraggi,[3] and Marco Guzzi[1]

[1]*Dipartimento di Fisica, Università del Salento, and INFN Sezione di Lecce, Via Arnesano 73100 Lecce, Italy*
[2]*Department of Physics and Institute of Plasma Physics University of Crete, 71003 Heraklion, Greece*
[3]*Department of Mathematical Sciences, University of Liverpool, Liverpool L69 7ZL, United Kingdom*

(Received 27 February 2008; published 16 July 2008)

Discovery potentials for extra neutral interactions at the Large Hadron Collider in forthcoming experiments are analyzed using resonant leptoproduction. For this purpose we use high precision next-to-next-to-leading order determinations of the QCD background in this channel, at the tail of the Drell-Yan distributions, in the invariant mass region around $0.8 < Q < 2.5$ TeV. We focus our analysis primarily on a novel string-inspired Z', obtained in left-right symmetric free fermionic heterotic string models and whose existence at low energies is motivated by its role in suppressing proton decay mediation. We analyze the parametric dependence of the predictions and perform comparison with other models based on bottom-up approaches, that are constructed by requiring anomaly cancellation and enlarged Higgs structure. We show that the results are not particularly sensitive to the specific charge assignments. This may render quite difficult the extraction of significant information from the forward-backward asymmetries on the resonance, assuming that these are possible due to a sizeable width. The challenge to discover extra (nonanomalous) Z' in this kinematic region remains strongly dependent on the size of the new gauge coupling. Weakly coupled extra Z' will not be easy to identify even with a very good theoretical determination of the QCD background through next-to-next-to-leading order.

DOI: 10.1103/PhysRevD.78.015012 PACS numbers: 11.25.Wx, 14.70.Hp

I. INTRODUCTION

The search for neutral currents mediated by extra gauge bosons (Z') at the Large Hadron Collider will gather considerable attention in the next few years [1]. Additional Abelian gauge interactions arise frequently in many extensions of the standard model, like in left–right symmetric models, in grand unified theories and in string-inspired constructions [1]. It has also been suggested that the existence of a low scale Z' may account for the suppression of proton decay mediating operators in supersymmetric theories and otherwise [2–4]. Abelian gauge structures may also play a considerable role in fixing the structure of the flavor sector, for instance, in pinning down the neutrinos mass matrix. Anomaly cancellation conditions, when supported also by an extended Higgs and fermion family structure—for instance, by the inclusion of right-handed neutrinos—may allow nonsequential solutions (i.e. charge assignments which are not proportional to the hypercharge) that are phenomenologically interesting and could be studied by ATLAS and CMS. Furthermore, within left-right symmetric models, and their underlying $SO(10)$ embedding, the global baryon minus lepton number ($B - L$) of the standard model is promoted to a local symmetry. Abelian gauge extensions are therefore among the most well-motivated extensions of the standard model. For these reasons, the identification of the origin of the extra neutral interaction in future collider experiments will be an important and challenging task. In particular, measurements of the charge asymmetries—both for the rapidity distributions and for the related total cross section—and of the forward-backward asymmetries, may be a way to gather information about the structure of these new neutral currents interactions, although in the models that we have studied this looks pretty difficult, given the low statistics.

As an extra Z' is common in model building, the differences among the various constructions may remain unresolved, unless additional physical requirements are imposed on these models in order to strengthen the possibility for their unique identification. In this work, we analyze the potential for the discovery of an extra Z' arising in a specific string construction, which is motivated not only by an anomaly free structure, as in most of the bottom-up models considered in the previous literature, but with some additional requirements coming from an adequate suppression of proton decay mediation. Bottom-up approaches based only on anomaly cancellation are, in this respect, less constraining compared with models derived either from a string construction or from theories of grand unification and can only provide a basic framework within which to direct the experimental searches. At the same time, the search for extra neutral interactions has to proceed in some generality and be unbiased, looking for resonances in several complementary channels. In this work, we will investigate the relation between more constrained and less constrained searches of extra neutral gauge bosons by choosing as a channel leptoproduction and proceed with a comparison of some proposals that have been presented in the recent literature. Our main interest is focused around an extra Z', which has been derived using the free fermionic formulation of string theory in a specific class of left-right symmetric string models. The new Abelian structure is determined not just

as an attempt to satisfy some additional physical requirements, on which we elaborate below, but is naturally derived from a class of string models that have been extensively studied in detail in the past two decades [5–8].

Our paper is organized as follows: in Sec. II, we discuss the origin of Z' in heterotic-string models. We discuss in some details the origin of the charge assignment under the Z', which is motivated from proton decay considerations and differs from those that have traditionally been discussed in the literature. Then, we move to define the conventions in regard to the charge assignments and the Higgs structure of the models that we consider, which are characterized by a gauge structure, which enlarges the gauge group of the standard model by one extra $U(1)$. Our numerical analysis of the invariant mass distributions for leptoproduction is performed by varying both the coupling of the extra $U(1)$ and the mass of the new gauge boson. The dependence on these parameters of the models that we discuss are studied rather carefully in a kinematic region, which can be accessed at the LHC. We compare these results with those obtained for a group of four different models, introduced in [9], for which we perform a similar analysis using leptoproduction. From this analysis it is quite evident that the search for extra neutral currents at the LHC is a rather difficult enterprise in leptoproduction, unless the coupling of the new gauge interaction is quite sizeable.

II. HETEROTIC–STRING-INSPIRED Z'

Phenomenological string models can be built in the heterotic string or, using brane constructions, in the type I string. The advantage of the former is that it produces states in spinorial representations of the gauge group, and hence allows for the $SO(10)$ embedding of the matter spectrum. The ten-dimensional supersymmetric heterotic-string vacua give rise to effective field theories that descend from the $E_8 \times E_8$ or $SO(32)$ gauge groups. The first case gives rise to additional Z's that arise in the $SO(10)$ and E_6 extensions of the standard model, and are the cases mostly studied in the literature [1]. A basis for the extra Z' arising in these models is formed by the two groups $U(1)_\chi$ and $U(1)_\psi$ via the decomposition $E_6 \to SO(10) \times U(1)_\psi$ and $SO(10) \to SU(5) \times U(1)_\chi$ [1]. Additional, flavor non-universal $U(1)$'s, may arise in heterotic $E_8 \times E_8$ string models from the $U(1)$ currents in the Cartan subalgebra of the four-dimensional gauge group, which are external to E_6. Non-universal Z's typically must be beyond the LHC reach, to avoid conflict with flavor changing neutral currents constraints. Recently [4], a novel Z' in quasirealistic string models that do not descend from the heterotic $E_8 \times E_8$ string has been identified. Under the new $U(1)$ symmetry left-handed components and right-handed components in the 16 spinorial $SO(10)$ representation, of each standard model generation, have charge $-1/2$ and $+1/2$, respectively. As a result, the extra $U(1)$ is family universal and anomaly free. It arises in left-right symmetric string models [8], in which the $SO(10)$ symmetry is broken directly at the string level to $SU(3) \times U(1)_{B-L} \times SU(2)_L \times SU(2)_R \times U(1)_{Z'} \times U(1)^n \times$ hidden [8]. The $U(1)^n$ are flavor dependent $U(1)$s that are broken near the string scale. The standard model matter states are neutral under the hidden sector gauge group, which in these string models is typically a rank 8 group. It is important to note that the fact that the spectrum is derived from a string vacuum that satisfies the modular invariance constraints, establishes that the model is free from gauge and gravitational anomalies. The pattern of $U(1)_{Z'}$ charges in the quasirealistic string models of Ref. [8] does not arise in related string models in which the $SO(10)$ symmetry is broken to the $SU(5) \times U(1)$ [5], the $SO(6) \times SO(4)$ [6], or $SU(3) \times SU(2) \times U(1)^2$ [7] subgroups. The reason for the distinction of the left-right symmetric string models is the boundary condition assignment to the world-sheet free fermions that generate the $SO(10)$ symmetry in the basis vectors that break the $SO(10)$ symmetry to one of its subgroups. The world-sheet fermions that generate the rank 8 observable gauge group in the free fermionic models are denoted by $\{\bar{\psi}^{1,\cdots,5}, \bar{\eta}^{1,2,3}\}$, where $\bar{\psi}^{1,\cdots,5}$ generate an $SO(10)$ symmetry, and $\bar{\eta}^{1,2,3}$ produce three $U(1)$ currents.[1] Additional observable gauged $U(1)$ currents may arise at enhanced symmetry points of the compactified six-dimensional lattice. The $SO(10)$ gauge group is broken to one of its subgroups $SU(5) \times U(1)$, $SO(6) \times SO(4)$, or $SU(3) \times SU(2) \times U(1)^2$ by the assignment of boundary conditions to the set $\bar{\psi}^{1\cdots5}_{1/2}$

$$\begin{aligned} &1.\ b\{\bar{\psi}^{1\cdots5}\bar{\eta}^{1,2,3}\} = \left\{\frac{1}{2}\frac{1}{2}\frac{1}{2}\frac{1}{2}\frac{1}{2}\frac{1}{2}\frac{1}{2}\frac{1}{2}\frac{1}{2}\frac{1}{2}\right\} \\ &\qquad\qquad \Rightarrow SU(5) \times U(1) \times U(1)^3, \\ &2.\ b\{\bar{\psi}^{1\cdots5}\bar{\eta}^{1,2,3}\} = \{11\,100\,000\} \\ &\qquad\qquad \Rightarrow SO(6) \times SO(4) \times U(1)^3. \end{aligned} \tag{1}$$

To break the $SO(10)$ symmetry to[2] $SU(3)_C \times SU(2)_L \times U(1)_C \times U(1)_L$ both steps 1 and 2, are used, in two separate basis vectors. The breaking pattern $SO(10) \to SU(3)_C \times SU(2)_L \times SU(2)_R \times U(1)_{B-L}$ is achieved by the following assignment in two separate basis vectors

$$\begin{aligned} &1.\ b\{\bar{\psi}^{1\cdots5}\bar{\eta}^{1,2,3}\} = \{11\,100\,000\} \\ &\qquad\qquad \Rightarrow SO(6) \times SO(4) \times U(1)^3, \\ &2.\ b\{\bar{\psi}^{1\cdots5}\bar{\eta}^{1,2,3}\} = \left\{\frac{1}{2}\frac{1}{2}\frac{1}{2}00\frac{1}{2}\frac{1}{2}\frac{1}{2}\right\} \\ &\qquad\qquad \Rightarrow SU(3)_C \times U(1)_C \times SU(2)_L \\ &\qquad\qquad\quad \times SU(2)_R \times U(1)^3 \end{aligned} \tag{2}$$

[1] For reviews and the notation used in free fermionic string models see, *e.g.* [10] and references therein.

[2] $U(1)_C = \frac{3}{2}U(1)_{B-L}$; $U(1)_L = 2U(1)_{T_{3_R}}$.

The distinction between the symmetry breaking patterns in Eqs. (1) and (2) is with respect to the charges of the standard model states under the three flavor dependent $U(1)$ symmetries $U(1)_{1,2,3}$ that arise from the three world-sheet fermions $\bar{\eta}^{1,2,3}$. In the free fermionic models, the states of each standard model generation fit into the 16 representation of $SO(10)$, and are charged with respect to one of the three flavor $U(1)$ symmetries. For the symmetry breaking pattern given in Eq. (1) the charge is always $+1/2$, i.e.

$$Q_j(16 = \{Q, L, U, D, E, N\}) = +\tfrac{1}{2}, \tag{3}$$

whereas for the symmetry breaking pattern in Eq. (2) the charges are

$$\begin{aligned} Q_j(Q_L, L_L) &= -\tfrac{1}{2} \\ Q_j(Q_R = \{U, D\}, L_R = \{E, N\}) &= +\tfrac{1}{2}. \end{aligned} \tag{4}$$

As a result in the models admitting the symmetry breaking pattern Eq. (1) the combination

$$U(1)_\zeta = U(1)_1 + U(1)_2 + U(1)_3 \tag{5}$$

is anomalous, whereas in the models admitting the symmetry breaking pattern (2) it is anomaly free. The distinction between the two boundary condition assignments given in Eqs. (1) and (2), and the consequent symmetry breaking patterns, is important for the following reason. Whereas the first is obtained from an $N = 4$ vacuum with $E_8 \times E_8$ or $SO(16) \times SO(16)$ gauge symmetry, arising from the $\{\bar{\psi}^{1,\cdots,5}, \bar{\eta}^{1,2,3}\bar{\phi}^{1,\cdots,8}\}$ world-sheet fermions, which generate the observable and hidden sectors gauge symmetries, the second cannot be obtained from these $N = 4$ vacua, but rather from an $N = 4$ vacuum with $SO(16) \times E_7 \times E_7$ gauge symmetry, where we have included here also the symmetry arising from the compactified lattice at the enhanced symmetry point. The important fact from the point of view of the Z' phenomenology in which we are interested is that the first case gives rise to the type of string-inspired Z' that arises in models with an underlying E_6 symmetry. Whereas the E_6 may be broken at the string level, rather than in the effective low energy field theory, the crucial point is that the charge assignment of the standard model states is fixed by the underlying E_6 symmetry. The entire literature on string-inspired Z' studies this type of E_6-inspired Z'. The second class, however, is novel and has not been studied in the literature. In this respect it would be interesting to examine how the symmetry breaking pattern (2), and the corresponding charge assignments (4) can be obtained in heterotic orbifold models in which one starts from a ten-dimensional theory and compactifies to four dimensions, rather than starting directly with a theory in four dimensions, as is done in the free fermionic models. This understanding may highlight the relevance of ten-dimensional backgrounds that have thus far been ignored in the literature. From the point of view of the Z' phenomenology, which is our interest here, the crucial point will be to resolve between the different Z' models and the fermion charges, which will reveal the relevance of a particular symmetry breaking pattern.

The existence of the extra Z' at low energies, within reach of the LHC, is motivated by proton longevity, and the suppression of the proton decay mediating operators [2–4]. The important property of this Z' is that it forbids dimension four, five, and six proton decay mediating operators. The extra $U(1)$ is anomaly free and family universal. It allows the fermions Yukawa couplings to the Higgs field and the generation of small neutrino masses via a seesaw mechanism. String models contain several $U(1)$ symmetries that suppress the proton decay mediating operators [3]. However, these are typically nonfamily universal. They constrain the fermion mass terms and hence must be broken at a high scale. Thus, the existence of a $U(1)$ symmetry that can remain unbroken down to low energies is highly nontrivial. The $U(1)$ symmetry in Refs. [4,8] satisfies all of these requirements. Furthermore, as the generation of small neutrino masses in the string models arises from the breaking of the $B - L$ current, the extra $U(1)$ allows lepton number violating terms, but forbids the baryon number violating terms. Hence, it predicts that R parity is violated and its phenomenological implications for supersymmetry collider searches differ substantially from models in which R–parity is preserved. The charges of the standard model states under the Z' are displayed in Table I. Also displayed in the table are the charges under $U(1)_{\zeta'} = U_C - U_L$, which is the Abelian combination of the Cartan generators of the underlying $SO(10)$ symmery that is orthogonal to the weak hypercharge $U(1)_Y$. The charges under the $U(1)$ combination given in Eq. (5) are displayed in Table I as well. These two $U(1)$'s are broken by the VEV that induces the seesaw mechanism, and the combination

TABLE I. Charge assignment for the free fermionic model.

Field	$U(1)_Y$	$U(1)_{\zeta'}$	$U(1)_\zeta$	$U(1)_{Z'}$
Q^i	$\frac{1}{6}$	$\frac{1}{2}$	$-\frac{1}{2}$	$\frac{3}{5}$
L^i	$-\frac{1}{2}$	$-\frac{3}{2}$	$-\frac{1}{2}$	$\frac{1}{5}$
U^i	$-\frac{2}{3}$	$\frac{1}{2}$	$\frac{1}{2}$	$-\frac{2}{5}$
D^i	$\frac{1}{3}$	$-\frac{3}{2}$	$\frac{1}{2}$	$-\frac{2}{5}$
E^i	1	$\frac{1}{2}$	$\frac{1}{2}$	0
N^i	0	$\frac{5}{2}$	$\frac{1}{2}$	0
ϕ^i	0	0	0	0
ϕ^0	0	0	0	0
H^U	$\frac{1}{2}$	-1	0	$-\frac{1}{5}$
H^D	$-\frac{1}{2}$	1	0	$\frac{1}{5}$
N_H	0	$\frac{5}{2}$	$\frac{1}{2}$	0
$\bar{N}_H$	0	$-\frac{5}{2}$	$-\frac{1}{2}$	0
ζ_H	0	0	1	1
$\bar{\zeta}_H$	0	0	-1	-1

$$U(1)_{Z'} = \frac{1}{5}U(1)_{\zeta'} - U(1)_{\zeta} \tag{6}$$

is left unbroken down to low energies in order to suppress the proton decay mediating operators. The charges of the standard model states under this $U(1)_{Z'}$ are displayed in Table I.

III. THE INTERACTIONS FOR $U(1)_{Z'}$

In this section, we fix our conventions and describe the structure of the new neutral sector that we are going to analyze numerically in leptoproduction afterwards. The notations are the same both in the case of the string model and for the other models that we will investigate. We show in Table I the field content of the string model obtained within the free fermionic construction discussed above. Of the three extra $U(1)$, we will decouple the two gauge bosons denoted by ζ, ζ' and keep only the Z'. The assumption of decoupling of these extra components are realistic if they are massive enough (> 5 TeV) so to neglect their influence on the lowest new resonance. We have chosen a mass $M_{Z'}$ around 0.8 TeV. We recall that a reasonable region where the new extra gauge boson have a chance of being detected is below the 5 TeV range.

The fermion-fermion- Z' interaction is given by

$$\sum_f z_f g_z \bar{f}\gamma^\mu f Z'_\mu, \tag{7}$$

where $f = e_R^j$, l_L^j, u_R^j, d_R^j, q_L^j and $q_L^j = (u_L^j, d_L^j)$, $l_L^j = (\nu_L^j, e_L^j)$. The coefficients z_u, z_d are the charges of the right-handed up and down quarks, respectively, while the z_q coefficients are the charges of the left-handed quarks. g_z is the Z' coupling constant. We can write the Lagrangian for the Z'-lepton-quark interactions as follows:

$$\begin{aligned}\mathcal{L}_{Z'} = \sum_j g_z Z'_\mu [&z_{e_R^j}\bar{e}_R^j\gamma^\mu e_R^j + z_{l_L^j}\bar{l}_L^j\gamma^\mu l_L^j + z_{u_R^j}\bar{u}_R^j\gamma^\mu u_R^j \\ &+ z_{d_R^j}\bar{d}_R^j\gamma^\mu d_R^j + z_{q_L^j}\bar{Q}_L^j\gamma^\mu Q_L^j],\end{aligned} \tag{8}$$

with j being the generation index. The low energy spectrum of the model, as discussed above, is assumed to be the same for the other models that we analyze in parallel. As shown in Table I, the field content of the model is effectively that of the standard model plus one additional Higgs doublet. The extra scalars ϕ, and ζ_H, $\bar{\zeta}_H$ and the right-handed components N_H and $\bar{N}_H$ are assumed to decouple. In this simplified framework, the structure of the vertex is the following:

$$-\frac{ig}{4\cos\theta_W}\bar{\psi}_i\gamma^\mu(g_V^{Z,Z'} + g_A^{Z,Z'}\gamma^5)\psi V_\mu, \tag{9}$$

where V_μ denotes generically the vector boson. In the standard model (SM)

$$\begin{aligned} v_u^\gamma &= \tfrac{2}{3} \qquad a_u^\gamma = 0 \qquad v_d^\gamma = -\tfrac{1}{3} \qquad a_d^\gamma = 0 \\ v_u^Z &= 1 - \tfrac{8}{3}\sin^2\theta_W \qquad a_u^Z = -1 \\ v_d^Z &= -1 + \tfrac{4}{3}\sin^2\theta_W \qquad a_d^Z = 1. \end{aligned} \tag{10}$$

We need to generalize this formalism to the case of the Z'.

Our starting point is the covariant derivative in a basis where the three electrically neutral gauge bosons W_μ^3, B_Y^μ, B_z^μ are

$$\begin{aligned}\hat{D}_\mu = \Big[&\partial_\mu - ig(W_\mu^1 T^1 + W_\mu^2 T^2 + W_\mu^3 T^3) \\ &- i\frac{g_Y}{2}\hat{Y}B_Y^\mu - i\frac{g_z}{2}\hat{z}B_z^\mu\Big]\end{aligned} \tag{11}$$

and we denote with g, g_Y, g_z the couplings of $SU(2)$, $U(1)_Y$ and $U(1)_z$, with $\tan\theta_W = g_Y/g$. After the diagonalization of the mass matrix we have

$$\begin{pmatrix} A_\mu \\ Z_\mu \\ Z'_\mu \end{pmatrix} = \begin{pmatrix} \sin\theta_W & \cos\theta_W & 0 \\ \cos\theta_W & -\sin\theta_W & \varepsilon \\ -\varepsilon\sin\theta_W & \varepsilon\sin\theta_W & 1 \end{pmatrix}\begin{pmatrix} W_\mu^3 \\ B_\mu^Y \\ B_\mu^z \end{pmatrix}, \tag{12}$$

where ε is defined as a perturbative parameter

$$\begin{aligned} \varepsilon &= \frac{\delta M_{ZZ'}^2}{M_{Z'}^2 - M_Z^2} \\ M_Z^2 &= \frac{g^2}{4\cos^2\theta_W}(v_{H_1}^2 + v_{H_2}^2)[1 + O(\varepsilon^2)] \\ M_{Z'}^2 &= \frac{g_z^2}{4}(z_{H_1}^2 v_{H_1}^2 + z_{H_2}^2 v_{H_2}^2 + z_\phi^2 v_\phi^2)[1 + O(\varepsilon^2)] \\ \delta M_{ZZ'}^2 &= -\frac{g g_z}{4\cos\theta_W}(z_{H_1}^2 v_{H_1}^2 + z_{H_2}^2 v_{H_2}^2). \end{aligned} \tag{13}$$

Then we define

$$g = \frac{e}{\sin\theta_W} \qquad g_Y = \frac{e}{\cos\theta_W}, \tag{14}$$

and we construct the $W^\pm$ charge eigenstates and the corresponding generators $T^\pm$ as usual

$$W^\pm = \frac{W_1 \mp iW_2}{\sqrt{2}} \qquad T^\pm = \frac{T_1 \pm iT_2}{\sqrt{2}}, \tag{15}$$

with the rotation matrix

$$\begin{pmatrix} W_\mu^3 \\ B_\mu^Y \\ B_\mu^z \end{pmatrix} = \begin{pmatrix} \frac{\sin\theta_W(1+\varepsilon^2)}{1+\varepsilon^2} & \frac{\cos\theta_W}{1+\varepsilon^2} & \varepsilon\frac{\cos\theta_W}{1+\varepsilon^2} \\ \frac{\cos\theta_W(1+\varepsilon^2)}{1+\varepsilon^2} & -\frac{\sin\theta_W}{1+\varepsilon^2} & \varepsilon\frac{\sin\theta_W}{1+\varepsilon^2} \\ 0 & \frac{\varepsilon}{1+\varepsilon^2} & \frac{1}{1+\varepsilon^2} \end{pmatrix}\begin{pmatrix} A_\mu \\ Z_\mu \\ Z'_\mu \end{pmatrix} \tag{16}$$

from the interaction to the mass eigenstates. Substituting these expression in the covariant derivative we obtain

$$\hat{D}_\mu = \Big[\partial_\mu - iA_\mu\Big(gT_3\sin\theta_W + g_Y\cos\theta_W\frac{\hat{Y}}{2}\Big) - ig(W_\mu^- T^- + W_\mu^+ T^+) - iZ_\mu\Big(g\cos\theta_W T_3 - g_Y\sin\theta_W\frac{\hat{Y}}{2} + g_z\varepsilon\frac{\hat{z}}{2}\Big) - iZ'_\mu\Big(-g\cos\theta_W T_3\varepsilon + g_Y\sin\theta_W\frac{\hat{Y}}{2}\varepsilon + g_z\frac{\hat{z}}{2}\Big)\Big], \tag{17}$$

where we have neglected all the $O(\varepsilon^2)$ terms. Sending $g_z \to 0$ and $\varepsilon \to 0$ we obtain the SM expression for the covariant derivative. The next step is to separate left and right contributions in the interactions between the fermions and the Z' boson. Hence, for the quarks and the leptons we can write an interaction Lagrangian of the type

$$\begin{aligned}\mathcal{L}_{\text{int}} = {} & \bar{Q}_L^j N_L^Z \gamma^\mu Q_L^j Z_\mu + \bar{Q}_L^j N_L^{Z'} \gamma^\mu Q_L^j Z'_\mu + \bar{u}_R^j N_{u,R}^Z \gamma^\mu u_R^j Z_\mu + \bar{d}_R^j N_{d,R}^Z \gamma^\mu d_R^j Z_\mu + \bar{u}_R^j N_{u,R}^{Z'} \gamma^\mu u_R^j Z'_\mu + \bar{d}_R^j N_{d,R}^{Z'} \gamma^\mu d_R^j Z'_\mu \\ & + \bar{Q}_L^j N_L^\gamma \gamma^\mu Q_L^j A_\mu + \bar{u}_R^j N_{u,R}^\gamma \gamma^\mu u_R^j A_\mu + \bar{d}_R^j N_{d,R}^\gamma \gamma^\mu d_R^j A_\mu + \bar{l}_L^j N_L^\gamma \gamma^\mu l_L^j A_\mu + \bar{e}_R^j N_{e,R}^\gamma \gamma^\mu e_R^j A_\mu + \bar{l}_L^j N_{L,\text{lep}}^Z \gamma^\mu l_L^j Z_\mu \\ & + \bar{l}_L^j N_{L,\text{lep}}^{Z'} \gamma^\mu l_L^j Z'_\mu + \bar{e}_R^j N_{e,R}^Z \gamma^\mu e_R^j Z_\mu + \bar{e}_R^j N_{e,R}^{Z'} \gamma^\mu e_R^j Z'_\mu,\end{aligned} \tag{18}$$

where for the quarks we have

$$\begin{aligned} N_L^{Z,j} &= -i\Big(g\cos\theta_W T_3^L - g_Y\sin\theta_W\frac{\hat{Y}^L}{2} + g_z\varepsilon\frac{\hat{z}^L}{2}\Big) \qquad N_L^{Z',j} = -i\Big(-g\cos\theta_W T_3^L\varepsilon + g_Y\sin\theta_W\frac{\hat{Y}^L}{2}\varepsilon + g_z\frac{\hat{z}^L}{2}\Big) \\ N_{u,R}^Z &= -i\Big(-g_Y\sin\theta_W\frac{\hat{Y}^{u,R}}{2} + g_z\varepsilon\frac{\hat{z}^{u,R}}{2}\Big) \qquad N_{d,R}^Z = -i\Big(-g_Y\sin\theta_W\frac{\hat{Y}^{d,R}}{2} + g_z\varepsilon\frac{\hat{z}^{d,R}}{2}\Big), \end{aligned} \tag{19}$$

and similar expressions for the leptons. We rewrite the vector and the axial coupling of the Z and Z' bosons to the quarks as

$$\begin{aligned} \frac{-ig}{4c_w}\gamma^\mu {g_V}^{Z,j} &= \frac{-ig}{c_w}\frac{1}{2}\Big[c_w^2 T_3^{L,j} - s_w^2\Big(\frac{\hat{Y}_L^j}{2} + \frac{\hat{Y}_R^j}{2}\Big) + \varepsilon\frac{g_z}{g}c_w\Big(\frac{\hat{z}_{L,j}}{2} + \frac{\hat{z}_{R,j}}{2}\Big)\Big]\gamma^\mu \\ \frac{-ig}{4c_w}\gamma^\mu\gamma^5 {g_A}^{Z,j} &= \frac{-ig}{c_w}\frac{1}{2}\Big[-c_w^2 T_3^{L,j} - s_w^2\Big(\frac{\hat{Y}_R^j}{2} - \frac{\hat{Y}_L^j}{2}\Big) + \varepsilon\frac{g_z}{g}c_w\Big(\frac{\hat{z}_{R,j}}{2} - \frac{\hat{z}_{L,j}}{2}\Big)\Big]\gamma^\mu\gamma^5 \\ \frac{-ig}{4c_w}\gamma^\mu {g_V}^{Z',j} &= \frac{-ig}{c_w}\frac{1}{2}\Big[-\varepsilon c_w^2 T_3^{L,j} + \varepsilon s_w^2\Big(\frac{\hat{Y}_L^j}{2} + \frac{\hat{Y}_R^j}{2}\Big) + \frac{g_z}{g}c_w\Big(\frac{\hat{z}_{L,j}}{2} + \frac{\hat{z}_{R,j}}{2}\Big)\Big]\gamma^\mu \\ \frac{-ig}{4c_w}\gamma^\mu\gamma^5 {g_A}^{Z',j} &= \frac{-ig}{c_w}\frac{1}{2}\Big[\varepsilon c_w^2 T_3^{L,j} + \varepsilon s_w^2\Big(\frac{\hat{Y}_R^j}{2} - \frac{\hat{Y}_L^j}{2}\Big) + \frac{g_z}{g}c_w\Big(\frac{\hat{z}_{R,j}}{2} - \frac{\hat{z}_{L,j}}{2}\Big)\Big]\gamma^\mu\gamma^5, \end{aligned} \tag{20}$$

where j is an index, which represents the quark or the lepton, and we have set $\sin\theta_W = s_w$, $\cos\theta_W = c_w$ for brevity.

The decay rates into leptons for the Z and the Z' are universal and are then given by

$$\begin{aligned} \Gamma(\mathcal{Z} \to l\bar{l}) &= \frac{g^2}{192\pi c_w^2} M_\mathcal{Z}[(g_V^{\mathcal{Z},l})^2 + (g_A^{\mathcal{Z},l})^2] = \frac{\alpha_{em}}{48 s_w^2 c_w^2} M_\mathcal{Z}[(g_V^{\mathcal{Z},l})^2 + (g_A^{\mathcal{Z},l})^2], \\ \Gamma(\mathcal{Z} \to \psi_i\bar{\psi}_i) &= \frac{N_c\alpha_{em}}{48 s_w^2 c_w^2} M_\mathcal{Z}[(g_V^{\mathcal{Z},\psi_i})^2 + (g_A^{\mathcal{Z},\psi_i})^2]\Big[1 + \frac{\alpha_s(M_\mathcal{Z})}{\pi} + 1.409\frac{\alpha_s^2(M_\mathcal{Z})}{\pi^2} - 12.77\frac{\alpha_s^3(M_\mathcal{Z})}{\pi^3}\Big], \end{aligned} \tag{21}$$

where $i = u, d, c, s$, and $\mathcal{Z} = Z, Z'$.

For the Z' and Z decays into heavy quarks we obtain

$$\begin{aligned} \Gamma(\mathcal{Z} \to b\bar{b}) &= \frac{N_c\alpha_{em}}{48 s_w^2 c_w^2} M_\mathcal{Z}[(g_V^{\mathcal{Z},b})^2 + (g_A^{\mathcal{Z},b})^2]\Big[1 + \frac{\alpha_s(M_\mathcal{Z})}{\pi} + 1.409\frac{\alpha_s^2(M_\mathcal{Z})}{\pi^2} - 12.77\frac{\alpha_s^3(M_\mathcal{Z})}{\pi^3}\Big], \\ \Gamma(\mathcal{Z} \to t\bar{t}) &= \frac{N_c\alpha_{em}}{48 s_w^2 c_w^2} M_\mathcal{Z}\sqrt{1 - 4\frac{m_t^2}{M_\mathcal{Z}^2}}\Big[(g_V^{\mathcal{Z},t})^2\Big(1 + 2\frac{m_t^2}{M_\mathcal{Z}^2}\Big) + (g_A^{\mathcal{Z},t})^2\Big(1 - 4\frac{m_t^2}{M_\mathcal{Z}^2}\Big)\Big] \\ &\quad \times\Big[1 + \frac{\alpha_s(M_\mathcal{Z})}{\pi} + 1.409\frac{\alpha_s^2(M_\mathcal{Z})}{\pi^2} - 12.77\frac{\alpha_s^3(M_\mathcal{Z})}{\pi^3}\Big]. \end{aligned} \tag{22}$$

The total hadronic widths are defined by

$$\Gamma_Z \equiv \Gamma(Z \to \text{ hadrons}) = \sum_i \Gamma(Z \to \psi_i \bar{\psi}_i)$$
$$\Gamma_{Z'} \equiv \Gamma(Z' \to \text{ hadrons}) = \sum_i \Gamma(Z' \to \psi_i \bar{\psi}_i), \tag{23}$$

where we refer to hadrons not containing bottom and top quarks (i.e. $i = u,\ d,\ c,\ s$). We also ignore electroweak corrections and all fermion masses with the exception of the top-quark mass, while we have included the relevant QCD corrections. Similarly to [9] we have considered only tree level decays into fermions, assuming that the decays into particles other than the SM fermions are either invisible or are negligible in their branching ratios, then the total decay rate for the Z and Z' is given by

$$\Gamma_Z = \sum_{i=u,d,c,s} \Gamma(Z \to \psi_i \bar{\psi}_i) + \Gamma(Z \to b\bar{b}) + 3\Gamma(Z \to l\bar{l}) + 3\Gamma(Z \to \nu_l \bar{\nu}_l)$$
$$\Gamma_{Z'} = \sum_{i=u,d,c,s} \Gamma(Z' \to \psi_i \bar{\psi}_i) + \Gamma(Z' \to b\bar{b}) + \Gamma(Z' \to t\bar{t}) + 3\Gamma(Z' \to l\bar{l}) + 3\Gamma(Z' \to \nu_l \bar{\nu}_l). \tag{24}$$

We also recall that the pointlike cross sections for the photon, the SM Z_0 and the new Z' gauge boson are written as

$$\sigma_\gamma(Q^2) = \frac{4\pi\alpha_{em}^2}{3Q^4}\frac{1}{N_c}$$
$$\sigma_Z(Q^2, M_Z^2) = \frac{\pi\alpha_{em}}{4M_Z \sin^2\theta_W \cos^2\theta_W N_c}\frac{\Gamma_{Z\to\bar{l}l}}{(Q^2 - M_Z^2)^2 + M_Z^2\Gamma_Z^2} \tag{25}$$
$$\sigma_{Z,\gamma}(Q^2, M_Z^2) = \frac{\pi\alpha_{em}^2}{6}\frac{(1 - 4\sin^2\theta_W)}{\sin^2\theta_W\cos^2\theta_W}\frac{(Q^2 - M_Z^2)}{N_C Q^2(Q^2 - M_Z^2)^2 + M_Z^2\Gamma_Z^2},$$

where N_C is the number of colors, and

$$\sigma_{Z'}(Q^2) = \frac{\pi\alpha_{em}}{4M_{Z'}\sin^2\theta_W\cos^2\theta_W N_c}\frac{\Gamma_{Z'\to\bar{l}l}}{(Q^2 - M_{Z'}^2)^2 + M_{Z'}^2\Gamma_{Z'}^2}$$
$$\sigma_{Z',\gamma}(Q^2) = \frac{\pi\alpha_{em}^2}{6N_c}\frac{g_V^{Z',l} g_V^{\gamma,l}}{\sin^2\theta_W\cos^2\theta_W}\frac{(Q^2 - M_{Z'}^2)}{Q^2(Q^2 - M_{Z'}^2)^2 + M_{Z'}^2\Gamma_{Z'}^2}, \tag{26}$$
$$\sigma_{Z',Z}(Q^2) = \frac{\pi\alpha_{em}^2}{96}\frac{[g_V^{Z',l} g_V^{Z,l} + g_A^{Z',l} g_A^{Z,l}]}{\sin^4\theta_W\cos^4\theta_W N_c}\frac{(Q^2 - M_Z^2)(Q^2 - M_{Z'}^2) + M_Z\Gamma_Z M_{Z'}\Gamma_{Z'}}{[(Q^2 - M_{Z'}^2)^2 + M_{Z'}^2\Gamma_{Z'}^2][(Q^2 - M_Z^2)^2 + M_Z^2\Gamma_Z^2]}.$$

The contributions such as Z, γ and similarly denote the interference terms. At LO (or leading order) the process proceeds through the $q\bar{q}$ annihilation channel and is $O(1)$ in the strong coupling constant α_s. The NLO (or next-to-leading order) corrections involve virtual corrections with one gluon exchanged in the initial state and real emissions involving a single gluon, which is integrated over phase space. These corrections are $O(\alpha_s)$ in the strong coupling. The change induced by moving from LO to NLO amounts to approximately 20 to 30% in the numerical value of the cross section that we consider. At the highest accuracy, we use in our analysis partonic contributions with hard scattering computed at next-to-next-to-leading order (NNLO), or $O(\alpha_s^2)$. At this order typical real emissions involve two partons in the final state—which are integrated over their phase space- and two-loop virtual corrections at the same perturbative order. The cross section for the invariant mass distributions factorizes at a perturbative level in terms of a NNLO or $O(\alpha_s^2)$ contribution W_V (which takes into account all the initial state emissions of real gluons and all the virtual corrections) and a pointlike cross section. The computation of W_V can be found in [11] to which we refer for more details. A similar factorization holds also for the total cross section if we use the narrow width approximation. At NLO or $O(\alpha_s)$). The color-averaged inclusive differential cross section for the reaction $p + p \to l_1 + l_2 + X$ is given by

$$\frac{d\sigma}{dQ^2} = \tau\sigma_V(Q^2, M_V^2)W_V(\tau, Q^2) \qquad \tau = \frac{Q^2}{S}, \tag{27}$$

where all the hadronic initial state information is contained in the hadronic structure function, which is defined as

$$W_V(\tau, Q^2) = \sum_{i,j}\int_0^1 dx_1 \int_0^1 dx_2 \int_0^1 dx\, \delta(\tau - x x_1 x_2) \times PD_{i,j}^V(x_1, x_2, \mu_F^2)\Delta_{i,j}(x, Q^2, \mu_F^2), \tag{28}$$

where the quantity $PD_{i,j}^V(x_1, x_2, \mu_F^2)$ contains all the information about the parton distribution functions and their evolution up to the μ_F^2 scale, while the functions $\Delta_{i,j}(x, Q^2, \mu_F^2)$ are the hard scatterings. This factorization formula is universal for invariant mass distributions medi-

ated by s-channel exchanges of neutral or charged currents. The hard scatterings can be expanded in a series in terms of the running coupling constant $\alpha_s(\mu_R^2)$ as

$$\Delta_{i,j}(x, Q^2, \mu_F^2) = \sum_{n=0}^{\infty} \alpha_s^n(\mu_R^2)\Delta_{i,j}^{(n)}(x, Q^2, \mu_F, \mu_R^2). \quad (29)$$

In principle, factorization and renormalization scales should be kept separate in order to determine the overall scale dependence of the results. However, as we are going to show, the high-end of the Drell-Yan distribution is not so sensitive to these higher order corrections, at least for the models that we have studied.

IV. NUMERICAL RESULTS

In our analysis, we have decided to compare our results with a series of models introduced in [9]. We refer to this work for more details concerning their general origin. It is worth noting that the construction of models with extra Z' using a bottom-up approach is, in general, rather straightforward, based mostly on the principle of cancellation of the gauge cubic $U(1)_{Z'}^3$ and mixed anomalies. One of the most economical ways to proceed is to introduce just one additional $SU(2)_W$ Higgs doublet and an extra scalar (weak) singlet, as in [12], and one right-handed neutrino per generation in order to generate reasonable operators for their Majorana and Dirac masses. However, more general solutions of the anomaly equations are possible by enlarging the fermion spectrum and/or enlarging the scalar sector [13]. In [9] the scalar sector is enlarged with two Higgs doublets and one (weak) scalar singlet.

Anomalous constructions, instead, require a different approach and several phenomenological analysis have been presented recently [14–17] that try to identify the signature of these peculiar realizations. In the anomalous models, due to the absence of the nonresonant behavior of the s channel (at least in the double prompt photon production), the chiral anomaly induces a unitarity growth, which should be present in correlated studies of other channels [17]. For nonanomalous Z' the phenomenological predictions are, as we are going to show, rather similar for all the models—at least in the mass invariant distributions in Drell-Yan—and the possibility to identify the underlying interaction requires a careful study of the forward-backward and/or charge asymmetries [18]. This is not going to be an easy task at the LHC, given the size of the cross section at the tail of the invariant mass distribution, the rather narrow widths, and given the presence of both theoretical and experimental errors in the parton distributions (pdf's), unless the gauge coupling is quite sizeable ($O(1)$). We refer to [19] for an accurate analysis of the experimental errors on the pdf's in the case of the Z peak. It has been shown that the errors on the pdf's are comparable with the overall reduction of the cross section as we move from the NLO to the NNLO.

These sources of ambiguities, known as experimental errors, unfortunately do not take into consideration the theoretical errors due to the implementation of the solution of the Dokshitzer-Gribov-Lipatov-Altarelli-Parisi in the evolution codes, which amount to a theoretical uncertainty [20]. Once all these sources of indeterminations are combined together, the expected error on the Z peak is likely to be much larger than 3%. Given the large amount of data that will accumulate in the first runs (for $Q = M_Z$), which will soon reduce the statistical errors on the measurements far below the 0.1% value, there will be severe issues to be addressed also from the theoretical side in order to match this far larger experimental accuracy. The possibility to use determinations of the pdf's on the Z peak for further studies of the Z' resonances at larger invariant mass values of the lepton pair, have to face several additional issues, such as the presence of an additional scale, which is $Q = M_{Z'}$, new respect to the $Q = M_Z$ scale used as a benchmark for partonometry in the first accelerator runs. We remind that logarithms of these two scales may also play a role especially if $M_{Z'}$ is far larger than M_Z. With these words of caution in mind we proceed with our exploration of the class of models that we have selected, starting from the string model and then analyzing the bottom-up models mentioned above [9]. These are studied in the limit $z_{H_1} = z_{H_2} = 0$, with the mass of the extra Z' generated only by the extra singlet scalar ϕ. In the string model, as one can see from Table I, only the two Higgses H_U and H_D contribute to the mass of the new gauge boson. The differences between these two types of models are, however, not relevant for this analysis, since the mass of the extra gauge boson is essentially a free parameter in both cases.

The set of pdf's that we have used for our analysis is MRST2001 [21], which is given in parametric form, evolved with CANDIA (see [22]). The models analyzed numerically are the free fermionic one, "F," discussed in the previous sections, and the "$B - L$," "$q + u$," "$10 + \bar{5}$" and "$d - u$," using the notations of [9].

Our results are organized in a series of plots on the various resonances and in some tables, which are useful in order to pin down the actual numerical value of the various cross sections at a given invariant mass.

A. $M_{Z'} = 0.8$ TeV

We show in Fig. 1 a plot of the Z' resonance around a typical value of 800 GeV for the FF model and the SM. The coupling of the extra neutral gauge boson is taken to be 0.05, with $\tan\beta = 10$. We remark that the dependence of the resonance on this second parameter is negligible. In fact, the relevant parameters are the coupling constant g_Z and the mass $M_{Z'}$. Notice that the width is very narrow (≈ 1 GeV) and basically invisible in an experimental analysis. Nevertheless, it is useful, for theoretical reasons, to try to characterize the signal and the background even in this (and other similar) unfavorable cases.

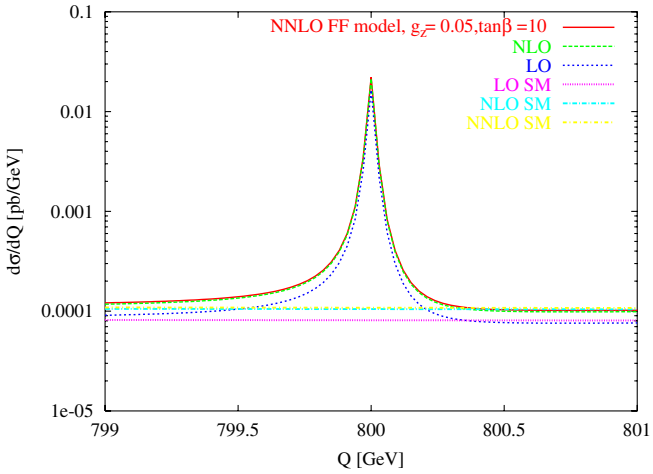

FIG. 1 (color online). Plot of the LO, NLO, and NNLO cross section for the free fermionic model with $M_{Z'} = 800$ GeV.

Assuming an integrated luminosity of 100 fb^{-1}/y after the first 3 years at the LHC (per experiment), we would expect 10 background events versus a signal of approximately 30 events. Notice that NLO and NNLO determinations of the cross section are, essentially, coincident for all practical purposes. We have checked that at larger values of Q around 1.2 TeV the determinations of the cross section in the free fermionic (FF) and SM models are basically overlapping as we move from LO to NLO and NNLO. Given the small size of the cross section ($\approx 10^{-2}$ fb) in this range, the possibility of resolving these differences experimentally is remote.

Looking at the mass invariant distributions, there are only minor differences between the four bottom-up models and the FF model. The FF model shows a resonance curve, which sits in the middle of all the determinations but is, for the rest, overlapping with the other curves. The "$B - L$" model, in all the cases, shows the widest width among all, with the "$q + u$" model following closely, while the "$d - u$" model has the narrowest one. This feature is quite apparent from Fig. 2(a) where the result is numerically smoothed out by the increased value of the coupling, which is now doubled compared with Fig. 2(b).

B. $M_{Z'} = 1.2$ and 2.5 TeV

We have illustrated in Fig. 3(a) and 3(b) our results for the various models for $M_{Z'} = 1.2$ TeV and 2.5 TeV. The QCD corrections are very small, and it is likely that the only role of these corrections, at these large Q values, is to stabilize the dependence of the perturbative series from the factorization/renormalization scales. In our case, we have chosen, for simplicity $\mu_F = \mu_R = Q$, where μ_R and μ_F are the renormalization and factorization scale, respectively. The separation of this dependence can be done as in [20], by relating the coupling constants at the two scales (μ_F, μ_R).

This separation, in general, needs to be done both in the hard scattering and in the evolution. Looking at the values in Table III we observe that the total cross sections are suppressed by a factor ≈ 10 and for a small value of g_z, as in the previous plots, we have small differences between the models $U(1)_{10-\bar{5}}$ and $U(1)_{d-u}$. Unlike the previous case ($M_{Z'} = 800$ GeV), the difference between $U(1)_{B-L}$ and $U(1)_{q+u}$ are reduced.

This drastic reduction of the cross section is one of the reason why the search of extra neutral currents, if these are mediated by new gauge bosons of mass above the 1 TeV range, may take several years of LHC luminosity to be performed, unless the new gauge coupling is larger. As we move away from the resonance region, the SM background and the FF result overlap. An interesting feature is that the K factors for the SM result are much larger with respect to the FF case, especially as we move from LO to NLO. We have shown, in Fig. 3(b) a plot of the shape of the reso-

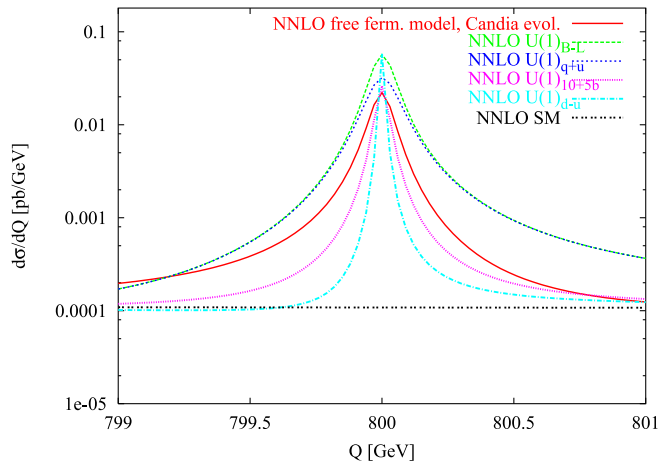

(a) $g_z = 0.1$

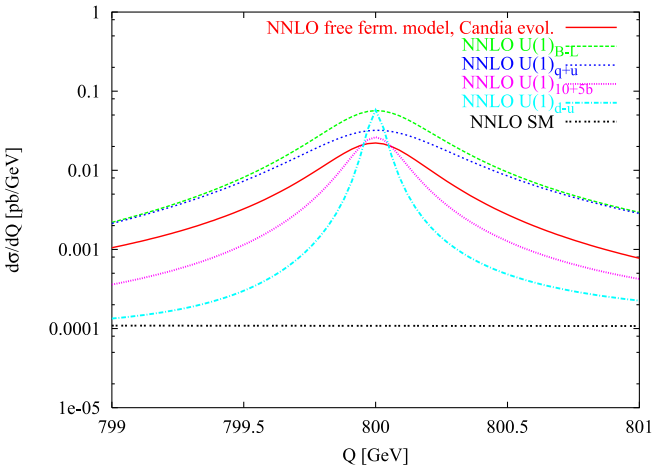

(b) $g_z = 0.2$

FIG. 2 (color online). Free fermionic model at the LHC $\tan\beta = 40$.

TABLE II. Total cross sections at NLO, $M'_Z = 800$ GeV.

$\sigma^{\rm nlo}_{\rm tot}$ [fb], $\sqrt{S} = 14$ TeV, $M_{Z'} = 800$ GeV, $\tan\beta = 40$, Candia evol.					
g_z	Free Ferm.	$U(1)_{B-L}$	$U(1)_{q+u}$	$U(1)_{10+\bar{5}}$	$U(1)_{d-u}$
0.1	2.957	8.239	6.223	1.899	1.949
	0.097	0.107	0.142	0.052	0.018
	0.041	1.026	0.582	0.053	0.082
0.3	26.671	74.734	58.683	16.906	12.457
	0.875	0.959	1.277	0.471	0.159
	0.365	9.303	5.484	0.476	0.521
0.5	73.967	205.937	155.390	47.035	34.586
	2.431	2.664	3.548	1.308	0.440
	1.013	25.635	14.522	1.325	1.447
0.7	144.957	403.272	304.296	92.135	67.784
	4.765	5.221	6.954	2.564	0.863
	1.985	50.200	28.439	2.595	2.836
1.0	296.192	822.281	620.129	188.019	138.318
	9.724	10.654	14.191	5.233	1.761
	4.057	102.359	57.956	5.295	5.786

nance region for $M_{Z'} = 2.5$ TeV. The width is very narrow (0.3 GeV) and the size of the cross section goes down by a factor of 100 compared with the case of $M_{Z'} = 1.2$ TeV. In Table IV, we repeat the previous analysis for $M_{Z'} = 2.5$ TeV, and we observe that the total cross sections are highly suppressed, while the total widths start to become large for $g_z = 0.7, 1$. As shown in Tables II, III, IV, and V, only at large values of the couplings the size of the width is such to ensure a more direct identification of the resonance, which should probably be around 30 GeV or more, in order not to be missed. We conclude this section with the discussion of some results concerning the study of the variation of the cross section $d\sigma/dQ(Q = M_{Z'})$ (on the peak) as we vary the factorization scale. If the scale μ_f is varied in the interval $1/2M_{Z'} < \mu_f < 2M_{Z'}$, these variations are rather small over all the energy interval that we have analyzed and show consistently the reduction of the scale dependence of the result moving from LO to NLO and NNLO (see the arXiv version for details). Finally, in Fig. 4 we plot the total cross section as a function of the energy for three values of the new gauge couplings for $M_{Z'} = 1.2$ TeV. Also, in this case the rise of the cross section becomes sizeable for larger value of the couplings.

C. Total cross sections

In Tables II and IV we perform a comparative study of all the models at the LHC up to NLO for three resonance masses of 800 GeV, 1.2 TeV, and 2.5 TeV.

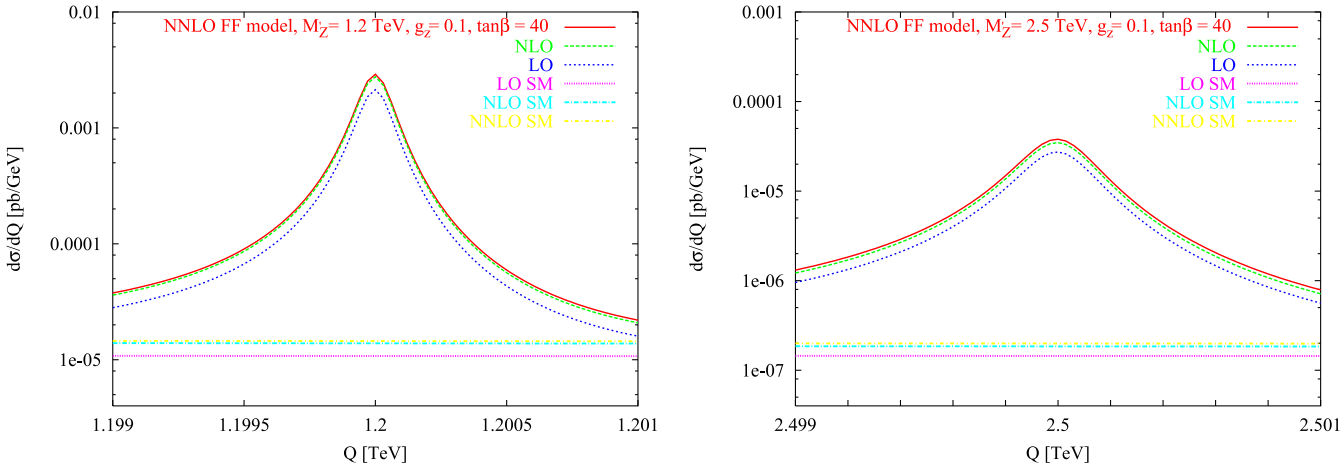

(a) $M_{Z'} = 1.2$ TeV (b) $M_{Z'} = 2.5$ TeV.

FIG. 3 (color online). Free fermionic model at the LHC $\tan\beta = 40$ and $g_z = 0.1$. Shown are also the SM results through the same perturbative orders.

TABLE III. Total cross sections at NLO, $M_{Z'} = 1.2$ TeV.

$\sigma_{\rm tot}^{\rm nlo}$ [fb], $\sqrt{S} = 14$ TeV, $M_{Z'} = 1.2$ TeV, $\tan\beta = 40$, Candia evol.					
g_z	Free Ferm.	$U(1)_{B-L}$	$U(1)_{q+u}$	$U(1)_{10+\bar{5}}$	$U(1)_{d-u}$
0.1	0.572	1.620	1.224	0.367	0.309
	0.146	0.160	0.213	0.079	0.027
	0.008	0.202	0.114	0.010	0.013
0.3	5.418	15.559	12.412	3.281	2.427
	1.314	1.439	1.916	0.715	0.240
	0.074	1.936	1.1160	0.091	0.101
0.5	14.316	40.465	30.535	9.149	6.741
	3.651	3.997	5.323	1.987	0.667
	0.195	5.036	2.853	0.255	0.279
0.7	28.077	79.270	59.836	17.915	13.212
	7.154	7.833	10.433	3.894	1.307
	0.383	9.865	5.591	0.498	0.547
1.0	57.394	161.625	121.921	36.556	26.959
	14.600	15.986	21.292	7.946	2.667
	0.783	20.114	11.392	1.017	1.117

In the first line of a single column for each model one can read the total cross section in $[fb]$, in the 2nd line the total width $\Gamma_{Z'}$ in GeV, and in the 3rd line the observable $\sigma_{\rm tot} \times BR(Z \to l\bar{l})$, where $BR(Z \to l\bar{l}) = \Gamma_{Z' \to l\bar{l}}/\Gamma_{Z'}$. These quantities refer to the value of the coupling constant g_z listed in the first column. To obtain the total cross section we have integrated the mass invariant distribution on the symmetric interval $[M_{Z'} - 3\Gamma_{Z'}, M_{Z'} + 3\Gamma_{Z'}]$. As we can observe from Table II, for $g_z = 0.1$ the two models $U(1)_{10+\bar{5}}$ and $U(1)_{d-u}$ show small differences in the total cross section while the free fermionic model, the $U(1)_{B-L}$ and the $U(1)_{q+u}$ models exhibit a clear difference. In all these models for $g_z = 0.1$ the total width is very small and this affects the quantity $\sigma_{tot} \times BR$. Increasing g_z the situation changes; in fact, we have different total cross sections, and we can better distinguish between the various models, but even when $g_z = 1$, the total width in the best case is around 10 GeV, thus it is very difficult to resolve it experimentally.

D. NLO/NNLO comparisons and relative differences

Analyzing the behavior of the mass invariant distributions in all the models (see Fig. 2), the proximity among the various determinations is quite evident, except on the resonance, where the values show wide variations. The pattern at NNLO is similar, and the changes in the cross sections from NLO to NNLO in most of the cases are around 3% or less. These changes are of the same order of those obtained by a study of the K factors in the case of

TABLE IV. Total cross sections at NLO, $M_{Z'} = 2.5$ TeV.

$\sigma_{\rm tot}^{\rm nlo}$ [fb], $\sqrt{S} = 14$ TeV, $M_{Z'} = 2.5$ TeV, $\tan\beta = 40$, Candia evol.					
g_z	Free Ferm.	$U(1)_{B-L}$	$U(1)_{q+u}$	$U(1)_{10+\bar{5}}$	$U(1)_{d-u}$
0.1	0.015	0.043	0.029	0.010	0.007
	0.304	0.333	0.444	0.167	0.056
	0.000	0.005	0.003	0.000	0.000
0.3	0.156	0.451	0.331	0.000	0.065
	2.735	2.997	3.992	1.501	0.503
	0.002	0.056	0.031	0.000	0.003
0.5	0.375	1.093	0.825	0.246	0.182
	7.598	8.324	11.088	4.170	1.397
	0.005	0.136	0.077	0.007	0.007
0.7	0.737	2.145	1.619	0.482	0.356
	14.893	16.316	21.732	8.172	2.737
	0.010	0.267	0.151	0.013	0.015
1.0	1.509	4.373	3.297	0.983	0.726
	30.394	33.298	44.350	16.678	5.586
	0.021	0.544	0.308	0.027	0.030

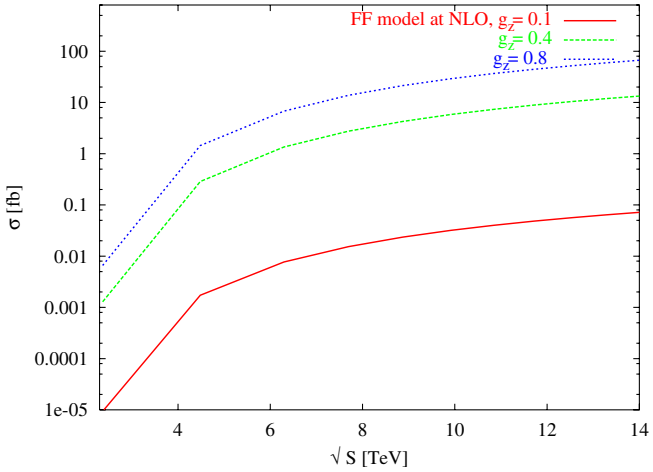

FIG. 4 (color online). Total cross section for the free fermionic model at NLO for three different values of g_z and for $M_{Z'} = 1.2$ TeV. Here, we have chosen $\mu_F = \mu_R = Q$ for simplicity, and we have integrated the mass invariant distribution on the interval $M_{Z'} \pm 3\Gamma_{Z'}$.

the Z resonance [20]. Also, for this kinematical region, as on the Z peak [20], the changes from LO to NLO are around 20–30%, and cover the bulk of the QCD corrections. Studying the relative differences between the results of the various models and the SM, at the various perturbative orders and for different values of the coupling constants we obtain an indication of the role played by the changes in the coupling on the behavior of these observables at the tails of the resonance region. It is rather clear that for a weakly coupled Z' ($g_Z = 0.05, 0.1$) the NLO and NNLO variations with respect to the SM result are essentially similar. The differences at NLO between the various models and the NLO SM are a fraction of a percent. Therefore, NNLO QCD corrections will not help in this region for such weakly coupled extra Z'. The differences are not more sizeable as we increase the new gauge coupling to 0.1. The differences between the SM and various models in the region of fast falloff can be of the order of only 2%, and just for one model ("$B - L$"). Given also the small size of these cross sections, which are of the order of 3×10^{-2} fb, it is hard to separate the various contributions. Naturally, the situation will improve considerably if we allow a larger gauge coupling, since the differences between signal and background can become, in principle, quite large. The differences among the predictions for the various models are more noticeable if we look at total cross sections, which we have obtained by integrating the invariant mass distributions around the peak. In this interval all the models exhibit differences in shape, width, and value at the peak of each distribution, which affect more significantly the inclusive observables (see Tables I, II, and III).

TABLE V. Dependence of the total width on the coupling constant g_z for the free fermionic model with $M_{Z'} = 800$ GeV, $M_{Z'} = 1.2$ TeV and $M_{Z'} = 2.5$ TeV.

$\Gamma_{M_{Z'}}(g_z)$ [GeV]			
g_z	$M_{Z'} = 0.8$ TeV	$M_{Z'} = 1.2$ TeV	$M_{Z'} = 2.5$ TeV
0.02	0.004	0.005	0.012
0.05	0.024	0.036	0.075
0.1	0.097	0.146	0.303
0.2	0.388	0.584	1.215
0.3	0.875	1.314	2.735
0.4	1.555	2.336	4.863
0.5	2.430	3.650	7.598
0.6	3.500	5.256	10.94
0.7	4.764	7.154	14.89
0.8	6.223	9.344	19.45
0.9	7.876	11.82	24.61
1	9.723	14.60	30.39

V. CONCLUSIONS

We performed a preliminary comparative analysis of the behavior of several models containing extra neutral currents in anomaly free constructions, and we discussed the implications of the results for actual experimental searches at the LHC. Compared with other studies, our objective has been to compare signal and QCD background in a series of models, with the highest accuracy, which can be systematically performed through NNLO. As expected, the critical parameters in order to be able to see a signal of these new interactions at the new collider are the size of the gauge coupling and the mass of the extra gauge boson, while the specific charge assignments of the models play a minor role. Other parameters such as $\tan\beta$ also do not play any significant role in these types of searches. It is reasonable to believe that much of the potentiality for discovering the new resonance, if found, is its width, and all the models analyzed so far show very similar patterns, with a gauging of $B - L$ being the one that has a slightly wider resonant behavior. Being the coupling so important in order to identify which model has better chances to be confirmed or ruled out, it is necessary, especially in bottom-up constructions, to rely on more precise investigations of possible scenarios for the running of the couplings, which are not addressed in approaches of these types. In the case of the free fermionic $U(1)$ that we have analyzed, the possibility to include these models in a more general scenario is natural, since they are part of a unification scheme, and a more complete analysis of these parameters could be pursued, but this is left for future studies. On the other hand, in these and similar models obtained either from string theory or from grand unified theories, the decoupling of part of the "extra stuff" that would complicate the scenario that we have analyzed, unfortunately requires extra assumptions, which would also affect the running of the couplings of the extra $U(1)'s$. These assumptions would introduce various alternatives on the choice of the symmetry breaking scales,

threshold enhancements, and so on, which amount, however, to important phenomenological details, which strongly affect this search.

Since the vector-axial structure of the couplings exhibits differences with respect to other Z' models a measurement of forward-backward asymmetries and/or of charge asymmetries could be helpful [18], but only if the gauge coupling is sizeable. The discrimination among the various models remains a very difficult issue for which NNLO QCD determinations, at least in leptoproduction, though useful, do not seem to be necessary in a first analysis. For those values of the mass of the extra Z' that we have considered these corrections cannot be isolated, while the NLO effects remain important. A more extensive analysis of the observables (mass invariant distributions up NNLO) presented in our study can be found in the ArXiv version of this work [23].

ACKNOWLEDGMENTS

We thank Simone Morelli for discussions and for various crosschecks in the numerical analysis. M. G. thanks the Theory Division at the University of Liverpool for hospitality and the Royal Society for financial support. The work of C. C. was supported (in part) by the European Union through the Marie Curie Research and Training Network Universenet Contract No. (MRTN-CT-2006-035863) and by The Interreg II Crete-Cyprus Program. He thanks the Theory group at Crete for hospitality. The work of A. E. F. is supported in part the STFC.

[1] For reviews and references therein see, e.g. P. Langacker, arXiv:0801.1345; T. G. Rizzo, arXiv:hep-ph/0610104; A. Leike, Phys. Rep. **317**, 143 (1999); Y. Y. Komachenko and M. Yu. Khlopov, Yad. Fiz. **51**, 1081 (1990); Sov. J. Nucl. Phys. **51**, 692 (1990).

[2] A. E. Faraggi and D. V. Nanopoulos, Mod. Phys. Lett. A **6**, 61 (1991); A. E. Faraggi, Phys. Lett. **499**, 147B (2001).

[3] J. Pati, Phys. Lett. B **388**, 532 (1996).

[4] C. Corianò, A. E. Faraggi, and M. Guzzi, Eur. Phys. J. C **53**, 421 (2008); H-S Lee, Phys. Lett. B **663**, 255 (2008).

[5] I. Antoniadis, J. Ellis, J. Hagelin, and D. V. Nanopoulos, Phys. Lett. B **231**, 65 (1989).

[6] I. Antoniadis, G. K. Leontaris, and J. Rizos, Phys. Lett. B **245**, 161 (1990).

[7] A. E. Faraggi, Phys. Lett. B **278**, 131 (1992); **274**, 47 (1992); Nucl. Phys. **B387**, 239 (1992); **B403**, 101 (1993); Phys. Rev. D **47**, 5021 (1993); Phys. Lett. B **377**, 43 (1996); Nucl. Phys. **B487**, 55 (1997); G. B. Cleaver, A. E. Faraggi, and D. V. Nanopoulos, Phys. Lett. B **455**, 135 (1999); Int. J. Mod. Phys. A **16**, 425 (2001); G. B. Cleaver, A. E. Faraggi, D. V. Nanopoulos, and J. W. Walker, Nucl. Phys. **B593**, 471 (2001); **B620**, 259 (2002); A. E. Faraggi, E. Manno, and C. Timirgaziu, Eur. Phys. J. C **50**, 701 (2007).

[8] G. B. Cleaver, A. E. Faraggi, and C. Savage, Phys. Rev. D **63**, 066001 (2001); G. B. Cleaver, D. J. Clements, and A. E. Faraggi, Phys. Rev. D **65**, 106003 (2002).

[9] M. Carena, A. Daleo, B. A. Dobrescu, and T. M. Tait, Phys. Rev. D **70**, 093009 (2004).

[10] A. E. Faraggi, Int. J. Mod. Phys. A **19**, 5523 (2004); arXiv: hep-th/9910042; arXiv:hep-ph/9707311.

[11] R. Hamberg, W. L. van Neerven, and T. Matsuura, Nucl. Phys. **B359**, 343 (1991); **644**, 403 (2002).

[12] T. Appelquist, B. A. Dobrescu, and A. R. Hopper, Phys. Rev. D **68**, 035012 (2003).

[13] H-S Lee, K. T. Matchev, and T. T. Wang, Phys. Rev. D **77**, 015016 (2008); Paul G. Langacker and Gil Paz Lian-Tao. Wang, Phys. Rev. Lett. **100**, 041802(2008); Phys. Rev. D**77**, 085033 (2008).

[14] C. Corianò, N. Irges, and S. Morelli, J. High Energy Phys. 07 (2007) 008.

[15] C. Corianò, N. Irges, and S. Morelli, Nucl. Phys. **B789**, 133 (2008).

[16] R. Armillis, C. Corianò, and M. Guzzi, J. High Energy Phys. 05 (2008) 015.

[17] C. Corianò, M. Guzzi, and S. Morelli, arXiv:0801.2949.

[18] F. Petriello and S. Quackenbush, Phys. Rev. D **77**, 115004 (2008).

[19] A. Cafarella, C. Corianò, and M. Guzzi, Nucl. Phys. **B748**, 253 (2006).

[20] A. Cafarella, C. Corianò, and M. Guzzi, J. High Energy Phys. 08 (2007) 030.

[21] A. D. Martin, R. G. Roberts, W. J. Stirling, and R. S. Thorne, Eur. Phys. J. C **23**, 73 (2002); Phys. Lett. B **531**, 216 (2002).

[22] http://www.le.infn.it/candia/.

[23] C. Claudio, A. Faraggi, and M. Guzzi, arXiv:0802.1792.